Spin-filter effect in metallic nanowires

N. Papanikolaou,[1] J. Opitz,[1] P. Zahn,[2] and I. Mertig[1]
[1]*Martin-Luther-Universität Halle, Fachbereich Physik, Fachgruppe Theoretische Physik, D-06099 Halle, Germany*
[2]*Fysiska Institutionen, Uppsala Universitet, Box 530, SE-75121 Uppsala, Sweden*
(Received 30 May 2002; published 31 October 2002)

We present *ab initio* calculations for metallic nanowires with a diameter of few atoms. The electronic structure is calculated using the screened Korringa Kohn Rostoker Green's function method, while electronic transport properties are obtained using a Green's function formulation of the Landauer formalism. We focus on the effect of scattering due to transition metal impurities on the conductance of a Cu wire. For a single defect, our results show a reduction of the transmission for energies at the impurity *d* state and due to the spin-polarization conductance is different for the two-spin directions causing a spin-filter effect. For a defect pair, quantum interference effects lead to a complicated energy dependence of the conductance.

DOI: 10.1103/PhysRevB.66.165441 PACS number(s): 73.63.Nm, 72.15.−v, 72.25.Ba

I. INTRODUCTION

Metallic atomic-size wires are interesting from technological as well as fundamental point of view. Conductors with a diameter of few nanometers could be used to connect the active electronic elements in future nanoelectronic devices.[1] However, electronic transport through wires with sizes comparable to the electron wavelength are still not well understood while a full quantum-mechanical description is necessary.

In nanometer dimensions electronic transport is mainly ballistic, and according to the Landauer formalism[2] conductance of a nanowire can be understood as electronic transport through channels. In the case of a two-point measurement the conductance of a wire is

$$g = \frac{2e^2}{h} \sum_{n=1}^{N} T_n , \tag{1}$$

with T_n the transmission probability of each channel n of the nanowire, while the factor 2 is for the two-spin directions.

Metallic nanocontacts have been fabricated by different methods like scanning tunneling microscope[3,4] or mechanically controllable break junctions.[5] There is a strong evidence that the conductance of these contacts is determined by the valence of the atoms in the constriction before the nanocontact breaks.[6] Moreover steplike changes of the conductance with the elongation of the nanocontact have been reported,[3–5] while a connection between structure and conductance variation was established experimentally in Au (Refs. 7,8) and Ag nanowires. The steplike behavior of the conductance upon elongation of the nanocontact is supported by the histogram distribution of a series of wire breaking experiments which show a peak near the conductance quantum $G_0=(2e^2/h)$, and smaller peaks at $2G_0$, $3G_0$, etc.[9] This is true for the noble metals but for transition-metal nanocontacts the situation is not yet clear.[10]

Metallic nanowires can also be fabricated using chemical methods by filling carbon nanotubes with metals[11] or using polymer templates which are filled with metals.[12] More recently, very thin Ag nanowire arrays[13] were produced using an organic matrix.

During the last years several groups have developed theoretical methods to calculate a nanocontact geometry.[3,14–18] The methods are usually tight binding,[19–21] but recently also *ab initio* density-functional theory calculations are reported for nanocontacts between jellium electrodes[14,15,17,18,22,23] while the conductance is calculated using the Landauer formalism.

The different behavior in transition-metal nanocontacts compared to noble metal ones has drawn attention to the behavior of alloy contacts.[10,24] A basic ingredient in order to understand these systems is to elucidate the way ballistic electrons are scattered at defects. Till now the theoretical study has concentrated on scattering by defects in carbon nanotubes[25] while Lang has calculated the effect of a sulfur atom in an aluminum chain connected to jellium electrodes.[15] Moreover, Brandbyge *et al.* used a jellium model to study the effect of scattering on the peak structure obtained in the break junction experiments. The conclusion was that the peak structure in the conductance histogram would survive even in the presence of defect scattering but the peak positions could be shifted.[26]

Diffusive transport in bulk dilute alloys is well studied over the years.[27] The residual resistivity is proportional to the strength of scattering. A rough estimation is given by a comparison of the local density of states of the host and the defect atom. On the other hand, in ballistic transport conductance is given by the transmission coefficients of the channels. For example, in a Cu wire the conductance is determined by the free-electron-like wire states at the Fermi level thus the presence of a defect will reduce transmission, due to scattering of the wire channels.

The main aim of this work is to study the influence of scattering by defects in nanowires using *ab initio* electronic structure calculations. The central question we address is how the wire free-electron-like conducting channels are scattered by impurities and, in particular, impurities with localized *d* orbitals. Is it possible to block channels of the Cu wire by localized *d* states? What is the influence of interference effects between defect atoms on the wire conductance? Answers to these questions will help to understand ballistic transport in wires with free-electron-like electronic states at the Fermi level, since conclusions can be generalized to Ag

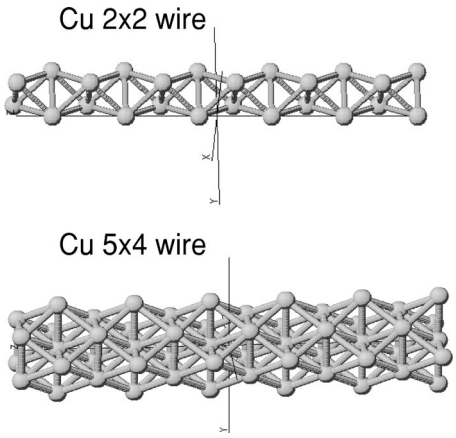

FIG. 1. Geometrical arrangement of the atoms in the 2×2 and 5×4 wires. The wires direction is (001) in a fcc lattice.

or Au nanowires that have similar electronic structure. Moreover it would be useful to investigate transport in alloy nanocontacts,[10] while the study of *d-sp* interference effects in ballistic conductors could help to understand also the spin transport in nanocontacts.

II. THEORY

The electronic structure was calculated using the screened KKR Green's function method, details of the method can be found elsewhere.[28] The angular momentum cut-off was $l_{max}=3$ for the wave functions and Green's function, while a multipole expansion of the charge density up to $l_{max}=6$ is taken into account. Exchange and correlation effects were described using the local density approximation to the density-functional theory[29] in the parametrization of Vosko Wilk Nusair.[30]

The structure of the wires is shown in Fig. 1. The wire direction is fcc (001), while for the 2×2 wire a supercell including two fcc (001) planes each having 16 sites was used to model the system. Two sites are occupied with Cu atoms while vacuum sites were used to separate the wires in the *xy* plane. Similarly two planes in fcc (001) direction having 25 sites each, were used to model the 5×4 wire. The distance between the Cu and the first nearest neighbors in the wires was taken to be the same as in bulk Cu with lattice constant 6.83 a.u. For simplicity, we did not allow for geometry optimization of the wires. The potential was restricted to a spherical shape (ASA) but nonspherical contributions in the charge density are included.

Within the screened KKR method (Ref. 28, and references therein) we obtain the Green's function of the ideal wire in two steps. First the screened structure constants $\mathbf{G}^r$ are obtained using a lattice of repulsive potentials of 4-Ry hight $\mathbf{V}^r$ as auxiliary reference system and solving a Dyson equation:

$$\mathbf{G}^r=\mathbf{g}^0+\mathbf{g}^0\mathbf{V}^r\mathbf{G}^r. \tag{2}$$

The free space Green's function $\mathbf{g}^0$ is known analytically.[28] Using the structure constants we can calculate the Green's function of the Cu wires $\mathbf{G}^{wire}$ for the potential $\mathbf{V}$ solving

$$\mathbf{G}^{wire}=\mathbf{G}^r+\mathbf{G}^r(\mathbf{V}-\mathbf{V}^r)\mathbf{G}^{wire}. \tag{3}$$

Due to periodicity Eq. (3) is solved in k space using 40 k-points in the wire direction. Once the perfect wire Green's function is known we can obtain the Green's function of a defect in the wire solving a Dyson equation in the vicinity of the defect

$$\mathbf{G}^{def}=\mathbf{G}^{wire}+\mathbf{G}^{wire}\Delta V\mathbf{G}^{def} \tag{4}$$

where ΔV is the potential difference between defect and ideal wire systems. The potentials of the defect plane and the first-neighbor planes are included in the self-consistent calculation.

Conductance g is calculated using the Kubo linear response formula as formulated by Baranger and Stone,[31] we consider a sample connected to two leads. Two surfaces C_n and C_m separate the leads from the sample. Following Ref. 31 the conductance between the two leads at the Fermi level E_F for zero temperature is given by

$$g=\frac{-e^2\hbar^3}{8\pi M^2}\int_{C_n}dS\int_{C_m}dS' G^+(\mathbf{r},\mathbf{r}';E_F)\overleftrightarrow{\nabla}\overleftrightarrow{\nabla}' G^-(\mathbf{r}',\mathbf{r};E_F), \tag{5}$$

where $f(r)\overleftrightarrow{\nabla}g(r)=f(r)\nabla g(r)-g(r)\nabla f(r)$, and G^+, G^- are the advanced and retarded Green's functions, respectively.

From the above Eq. (5) it is clear that an integral over two surfaces in the left and right lead have to be performed. Within the ASA we consider integrals over atomic planes. Using the usual site-angular momentum expansion for the Green's function[28]

$$G(\mathbf{r}+\mathbf{R}^n,\mathbf{r}'+\mathbf{R}^{n'};E)=\delta_{nn'}\sqrt{E}\sum_L R^n_L(\mathbf{r}_<;E)H^n_L(\mathbf{r}_>;E) + \sum_{LL'} R^n_L(\mathbf{r};E)G^{nn'}_{LL'}(E)R^{n'}_{L'}(\mathbf{r}';E), \tag{6}$$

where R^n_L, H^n_L are regular and irregular solutions of the Schröndinger equation for the potential at site n, and $G^{nn'}_{LL'}(E)$ is the structural Green's function matrix, connecting the scattering events of sites n and n'. Taking the wire direction to be along the z axis and the two planes perpendicular to it we derive the final formula for the conductance in the wire,

$$g=\frac{-e^2\hbar^3}{8\pi M^2}\sum_{nm}\sum_{L'L''}\sum_L (J^n_{LL''}-J^{*n}_{L''L}) \times G^{nm}_{LL'}\sum_{L'''}(J^m_{L'L'''}-J^{*m}_{L'''L'})G^{*nm}_{L''L'''}. \tag{7}$$

The star denotes complex conjugate, and we have dropped the energy dependence. The sum in m runs over all atoms on

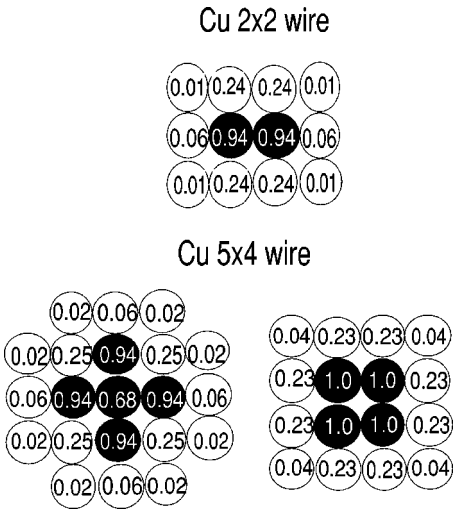

FIG. 2. Conductance distribution in the wires cross sections. For a 2×2 wire the conductance is $3G_0$ while for the 5×4 we find $6G_0$. Atoms occupy the full circles position, empty circles mean vacuum sites. For the 5×4 wire we have two cross sections (look at Fig. 1).

the plane connecting to the right lead while the *n* sum is over the atoms on the plane connecting the left lead. The matrix elements are given by

$$J_{LL'}=\frac{1}{\Delta}\int_{WS} d^3r R_L(\mathbf{r})\partial_z R^*_{L'}(\mathbf{r}), \tag{8}$$

where Δ is the distance separating two nearest-neighbor atomic planes in *z* direction, and the integration is over the Wigner-Seitz cell.

A detailed derivation together with the advantages of this approach will be discussed elsewhere.[32] The Green's function was calculated using an energy with a small imaginary part ImE$=0.04$ mRy. Convergence is reached using 20.000 points in the wire one-dimensional Brillouin zone for the calculation of the host-wire Green's function. The angular momentum cut-off $l_{max}=3$ was also checked, increase to $l_{max}=4$ did not change our results significantly.

III. RESULTS DISCUSSION

A. Ideal wires

The conductance of a nanowire with a diameter of few atoms is ballistic, and according to the Landauer formula [Eq. (1)], the conductance is just the sum of the states in the leads weighted with the transmission probability. In an infinite, one-dimensional, periodic wire the transmission probability of the states is always unity, which means that the conductance is just the number of states at the Fermi energy. The total conductance is expressed as a sum over all pairs of atoms from the left to the right plane in the leads [Eq. (7)]. Summing all contributions on one side we can get the spatial distribution of the conductance. This is shown in Fig. 2 for both the 2×2 and 5×4 wires. The total conductance of the 2×2 wire is $3G_0$, and for the 5×4 wire we obtain six channels, which is the number of bands that cross the Fermi level. For the thinner wire the conductance contribution going through the atoms is close to two channels while the spill-out of the wave function in the vacuum gives roughly one more channel. For the 5×4 wire we have two cross sections, again there is significant contribution from the vacuum region. The current through the different cross sections sums up to the same value. We have also calculated a thicker 16×9 wire and conductance was found to be 13 channels. The conductance distribution depends on the symmetry of the wave function at the Fermi level. In the limit of very thick wires the ballistic conductance per atom will approach the value of Cu bulk (001) which is approximately 0.91 channels per atom. We note that in case of bulk, the ballistic conductance is just the area of the Fermi surface projected along the (001) direction.

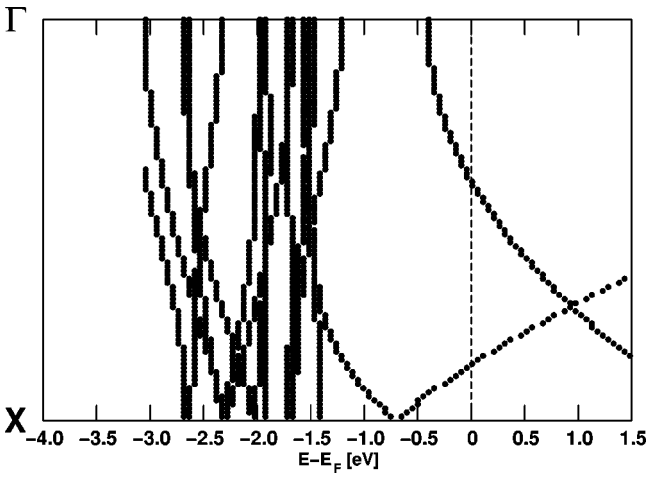

FIG. 3. Band structure of the Cu 2×2 wire close to the Fermi level.

To conclude our discussion on the infinite wires we present in Fig. 3 the band structure of the Cu 2×2 wire. At the Fermi level we have three bands crossing, one nondegenerate band close to the *X* point and a double-degenerate band, which starts around 0.4 eV below the Fermi level. In fact, this degeneracy is lifted in the case of a 2×2 Cu (110) wire but our calculations show that the number of conducting channels at the Fermi level remains three. Moreover in Fig. 4 we present the orbital decomposed density of states of a Cu site in the 2×2 wire. The one-dimensional character is observed in the characteristic $(1/\sqrt{E})$ shape of the density of states close to the van Hove singularity at around -0.4 eV. The band structure of a (110) 2×2 Cu wire is qualitatively the same as the band structure of an infinite Ag wire[13] in (110) direction.

B. Single defects

After the infinite, ideal wires we proceed now to study scattering by defects. We concentrate on the thinner Cu 2×2 wire and consider first a single substitutional impurity. The perturbation in the region around the defect atom is calculated self-consistently in real space, using the ideal wire as host reference. The perturbation is extended to 36 sites in the vicinity of the impurity atom, we consider Ti, V, Cr, Mn,

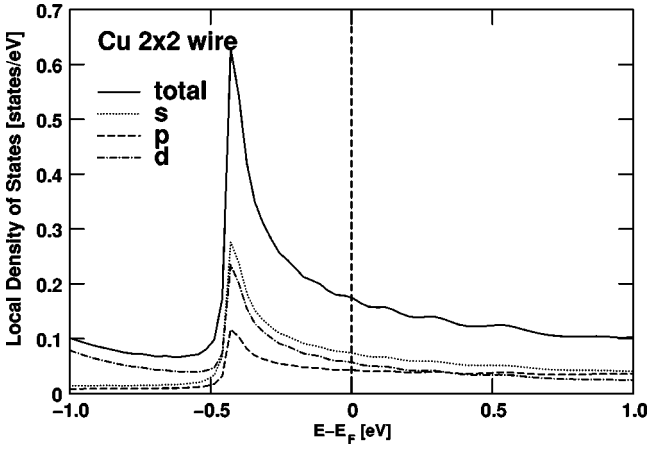

FIG. 4. Local density of states for the Cu 2×2 wire close to the Fermi level.

Fe, Co, Ni, and Zn impurities. Within the local-density approximation the impurities develop a strong spin splitting when embedded in the wire, and the local magnetic moments were found to be 0.65 for Ti, 2.85 for V, 4.06 for Cr, 4.22 for Mn, 3.14 for Fe, and 1.85 for Co in μ_B. For Ni and Zn the ground state was paramagnetic.

The conductance was calculated taking two planes outside the defect region in the ideal left and right lead. In the case of an infinite wire the available states are only the wire states, so introducing an impurity will reduce the wire conductance. In our Cu 2×2 wire we expect a maximum value of $3e^2/h$ per spin. Our calculations for the conductance at the Fermi level for a wire with defects are shown in Fig. 5. Scattering by impurities has a strong influence on the transport properties. For the majority (spin-up) channel we see a strong reduction of g in the beginning of the series in Ti and V, and values only slightly smaller than $3e^2/h$ towards the end of the d series with the exception of Ni. In the minority (spin-down) channel we find only a small reduction of g in the beginning of the $3d$ series, while with increasing atomic number, for Fe, Co, and Ni we observe strong scattering, and thus conductance reduction.

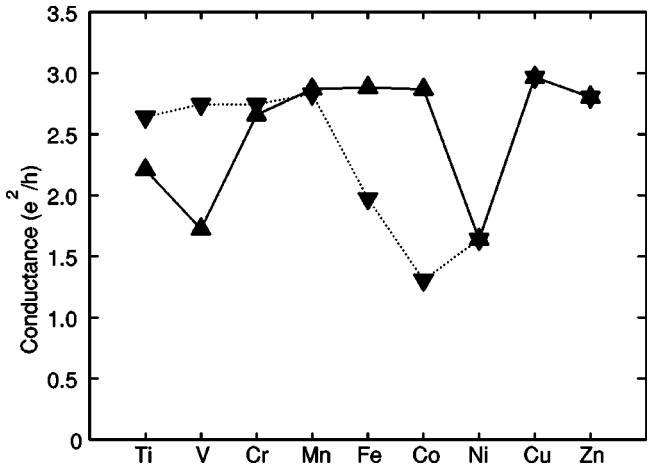

FIG. 5. Conductance for different substitutional impurities in the Cu 2×2 wire at the Fermi energy. Up triangles are for majority, down triangles for minority spins. The lines are to guide the eye, full line majority spin, dashed line minority spin.

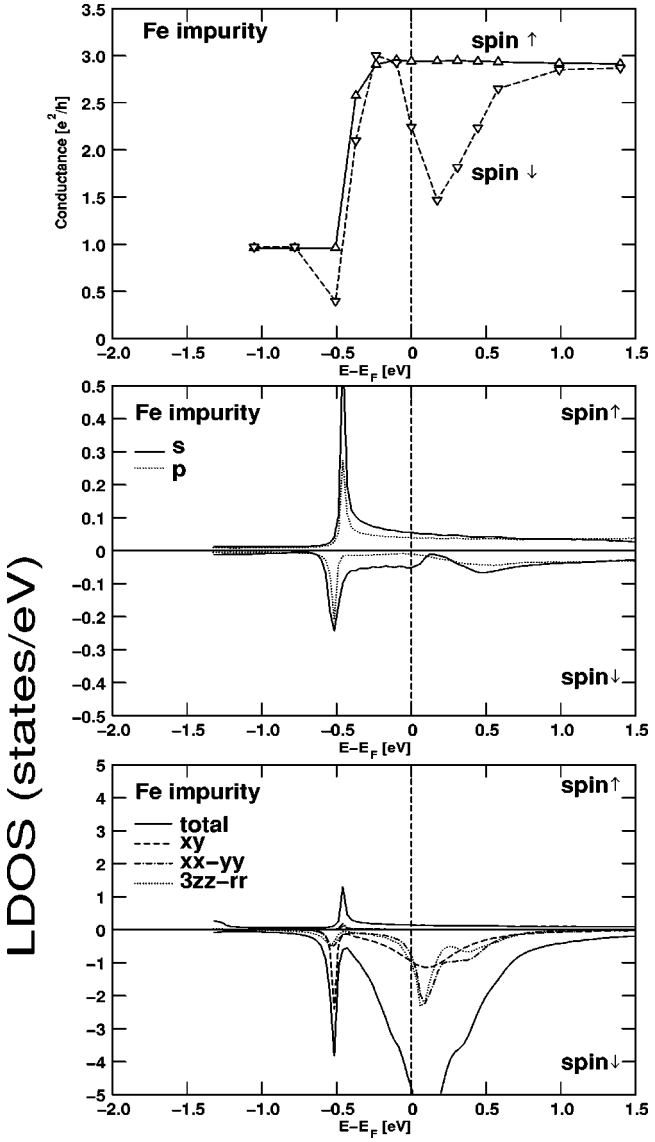

FIG. 6. Energy variation of the conductance for an Fe single impurity in the Cu 2×2 wire (upper panel), together with orbital decomposed local density of states (LDOS), s and p orbitals (middle panel), and d orbitals parallel to the wire direction $d_{3z^2-r^2}$, perpendicular to the wire direction d_{xy} and $d_{x^2-y^2}$ together with the total LDOS. Both majority (up) and minority (down) spin are shown.

In order to understand the behavior of the conductance, it is important to study the energetic positions of the d states with respect to the Fermi level. In Fig. 6 we plot the conductance variation with the energy in comparison with the orbital decomposed local density of states (LDOS) at the impurity site. We show the s and p contribution in the middle panel, while in the lower panel we decompose the total LDOS in d orbitals only along the wire direction $d_{3z^2-r^2}$, and d orbitals only perpendicular to the wire direction d_{xy} and $d_{x^2-y^2}$ which are shown together with the total LDOS.

We have chosen to focus on the Fe impurity in detail, however, the conclusions would be similar for any other transition-metal defect.

We first concentrate on the LDOS of the majority channel (spin-up), shown in the middle and lower panels of Fig. 6. The Fe spin-up *d* states are not shown in the figure since they are occupied and below -1.5 eV in energy. In the energy window close to E_F, we observe only a sharp peak on the *sp* LDOS at -0.4 eV (middle panel). This peak is induced by the van Hove singularity of the Cu wire at the bottom of the double-degenerate band (compare Figs. 3, 4) and it was seen also in the ideal wire LDOS. This has a direct consequence in the majority spin conductance where we have a jump from one to three channels at this energy.

For minority (down) spin the behavior is more complicated. First, in the *d*-band region just above the Fermi level we observe a depletion of the *s* band, together with a sharp drop of the conductance. Moreover, at the wire van Hove singularity, the impurity wave function is localized perpendicular to the wire direction which is manifested by a peak of the d_{xy} orbital, accompanied with a drop in *g*. It is interesting to investigate the bandwidth of the different orbitals since the behavior for the other impurities is similar. As seen in Fig. 6 the in-wire-direction $d_{3z^2-r^2}$ orbital forms a narrow resonance, which is just above E_F for Fe. The orbital perpendicular to the wire-direction $d_{x^2-y^2}$ forms a similar narrow resonance at the same energy, while d_{xy} shows a much broader resonance at the same energy region. This behavior is quite similar for all the other *d* impurities. The only difference is the energetic position of the *d* resonances that move to lower energies with increasing atomic number.

A drop in the conductance is observed in the position of the *d* resonance and this is accompanied by a depletion of the *s* band. This is seen for Fe at around $+0.2$ eV above the Fermi level (Fig. 6). By reducing valence, going from Ni to Co, Fe and Mn the conductance minimum is shifted to higher energies. For Ni the conductance minimum is found around -0.4 eV, while for Co the minimum is at the Fermi level, and for Mn at around $+0.6$ eV. This effect is repeated for the majority band as the *d* band crosses the Fermi level, and this explains the conductance drops for Ti and V in the majority band.

The variation of conductance within the $3d$ series seen in Fig. 5 can now be explained. For the early elements the *d* resonance is close to E_F for the spin-up channel, so we have a depletion of the s band and a reduction of *g* for Ti and Cr. For impurity atoms from the middle of the series no *d* states are present in the vicinity of the Fermi level due to the spin splitting, and only a small reduction is observed in conductance. The minority *d* band comes close to the Fermi level again for Fe, Co, and Ni and this reduces *g* for the spin-down electrons as seen in Fig. 5.

Here we should note that we cannot make a direct comparison between our results and the break junction experiments where a reservoir of bulk states is available. There is evidence[6] that in the break junction experiment conductance will scale with the number of valence electrons of the last atom that connects the junction before it breaks. The results presented here are not in contradiction with this experimental finding, but our study is valid only for defects in a wire which is long enough so that the conducting states are close to the states of an infinite wire.

The effect of impurity atoms in metallic wires was studied previous by Lang[15] who investigated the effect of an *sp*-sulfur impurity atom in an Al wire. He attributed the drop in the conductance to the change in the LDOS at the Fermi level. The situation changes for transition-metal impurities. In the case of localized *d* electrons it is more appropriate to compare the conductance with the free-electron-like states, which have mainly *s* character since *d* states dominate the LDOS, but they do not give the major contribution in conductance. Actually, a drop in the conductance is often accompanied by a reduction of the *s* LDOS. The reasoning is simple. In ballistic conductance essentially *sp* electrons of high velocity dominate the conducting channels, reducing the number of *s* electrons with an impurity atom will reduce the states that carry the current, and conductance will drop due to this bottleneck.

From Fig. 6 we see that the drop in the conductance occurs at the energetic position of the minority spin *d* state, additionally we observe a drop of the *s* LDOS at the same energy region. However, there is no one to one quantitative correspondence between the *s* DOS or the total LDOS and the conductance. This is different compared to systems with *sp* electrons like C nanotubes[33,34] where conductance variation with energy follows the LDOS change.

Our results show that it is possible to reduce the conductance of a nanowire by introducing atoms with localized electrons. Some recent experimental evidence from break junction experiments with CuCo, AuPd, and CuNi alloys[10,24] showed only a smoothening of the peak structures. However, break junction experiments are probably not so appropriate to resolve such effects since the results for individual impurities can be greatly influenced by quantum interference between the impurity atoms. This will be discussed in the following section. Moreover, *sp* scattering alone can also reduce the conductance.

C. Defect pairs

In order to investigate the effect of a higher concentration of impurities in a wire and to estimate the importance of quantum interference effects between them, we consider systems with two substitutional impurity atoms. The two impurities occupy the two sites in the same plane perpendicular to the wire direction (see Fig. 1) thus the Cu 2×2 wire is ''broken'' by the defect pair. We consider again the same series of defect pairs, and with the exception of Ni and Zn all pairs were found to be spin polarized. The magnetic moments are similar to that of the single defects and typically $0.1\ \mu_B$ smaller.

The results for the conductance are shown in Fig. 7. The behavior of *g* across the $3d$ series is rather different compared to the single-defect case. In the majority-spin channel the major feature is a significant drop in Ti and Cr from $3e^2/h$ to almost $2e^2/h$, while Ni is spin degenerate and causes also a strong reduction of the transmission. For the other defects we observe only a small reduction. For the

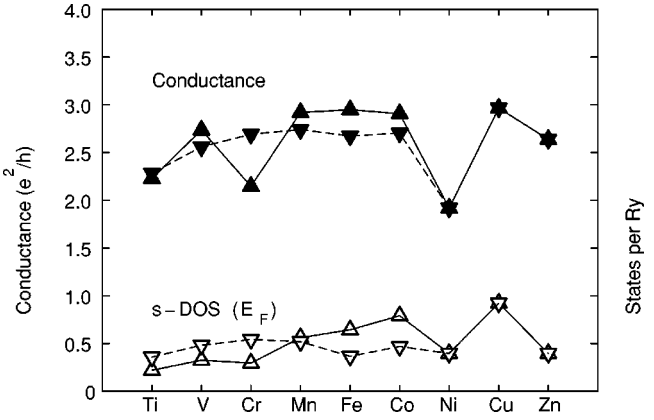

FIG. 7. Conductance for different impurity pairs in the Cu 2 $\times$2 wire at the Fermi energy (full symbols), together with the *s* DOS at the Fermi level (empty symbols). Up triangles are for majority, down triangles for minority spin. The lines are to guide the eye, full line majority spin, dashed line minority spin.

majority-spin electrons we have a rather smooth behavior with the exception of Ni. All impurities seem to cause a small drop of the conductance which is quite significant in the beginning of the series for Ti and becomes smaller with increasing atomic number. Comparing Fig. 7 and 5, it becomes clear that quantum interference between the defects has a strong impact on the channel transmission. Interestingly, the trend for the impurity pairs with the exception of Ni and Cr can be explained by considering that the transition-metal impurities act only as *s*-scattering centers. This can be simulated by calculating the conductance through artificial scatterers that have only the *s*-phase shift of the impurity and setting all other phase shifts to the Cu wire ones.

From Fig. 7 we see that there is also a reasonable correlation with the *s* LDOS, and we could predict the drop for Ni and Zn pairs, as well as the reduction of conductance going from Mn to Cr in the majority band by just comparing the *s* LDOS. However, quantitative comparison is not as good since, for example, Ni and Co minority have similar *s* LDOS, but large difference in g.

We can learn more by studying again the energy dependence of the conductance and compare it to the orbital decomposed LDOS. Results are shown in Fig. 8 for the case of an Fe pair, and they can be compared directly to the single-impurity case shown in Fig. 6. Conductance variation is simple for the majority channel and very similar to the impurity case. For the minority channel we observe a slower increase with g reaching values close to $3e^2/h$ channels and a sharp drop to $2e^2/h$ at around 0.6 eV above the Fermi level. Conductance increases back to three around 1.5 eV. As we can see in the LDOS, the impurity pair causes a splitting in bonding and antibonding orbitals for the d states. The splitting is different for each orbital and this causes the complicated conductance variation with energy. Comparing with Fig. 6, we see that since we consider the impurity pair perpendicular to the wire direction the $d_{3z^2-r^2}$ is not splitted but shifted to slightly higher energy. The splitting in the in-plane orbitals has mainly two effects. First a broad $d_{x^2-y^2}$ bonding

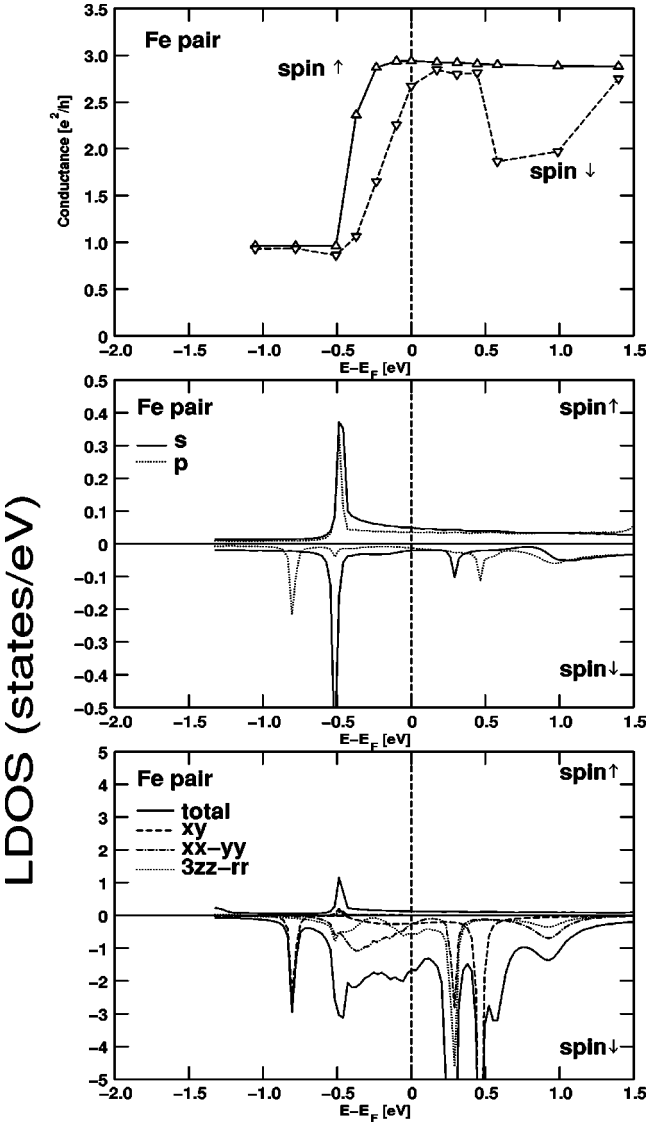

FIG. 8. Same as in Fig. 6 but for an Fe pair in the Cu 2$\times$2 wire.

state appears at -0.3 eV, below the Fermi level and it is accompanied with a depletion of the $d_{3z^2-r^2}$ orbitals. This is responsible for the behavior of the conductance of the minority band just below E_F. Contrary to the case of one Fe impurity (Fig. 6), g has no sharp transition from one to three at -0.4 eV, but increases slowly to reach the value of three only close to the Fermi level. Moreover, just above the Fermi level for one impurity we have seen a big drop in conductance, while due to interference effects no reduction is seen for the pair. This is reflected also in the *s* states that show a peak at the position of the $d_{3z^2-r^2}$ resonance. For higher energies around $+0.9$ eV conductance drops since, the in-plane orbitals dominate again, and the *s* LDOS reduces.

The behavior is similar for the other impurity pairs. We present only the energy variation of the conductance for pure Cu wire, together with Ni, Co, and Mn pairs in Fig. 9. In the majority channel for Co we see a sharp transition from one to three channels at -0.4 eV. For Mn the increase is smoother. This is characteristic of *s* scattering and it is also seen in Zn. On the other hand the result of Ni is caused by the scattering

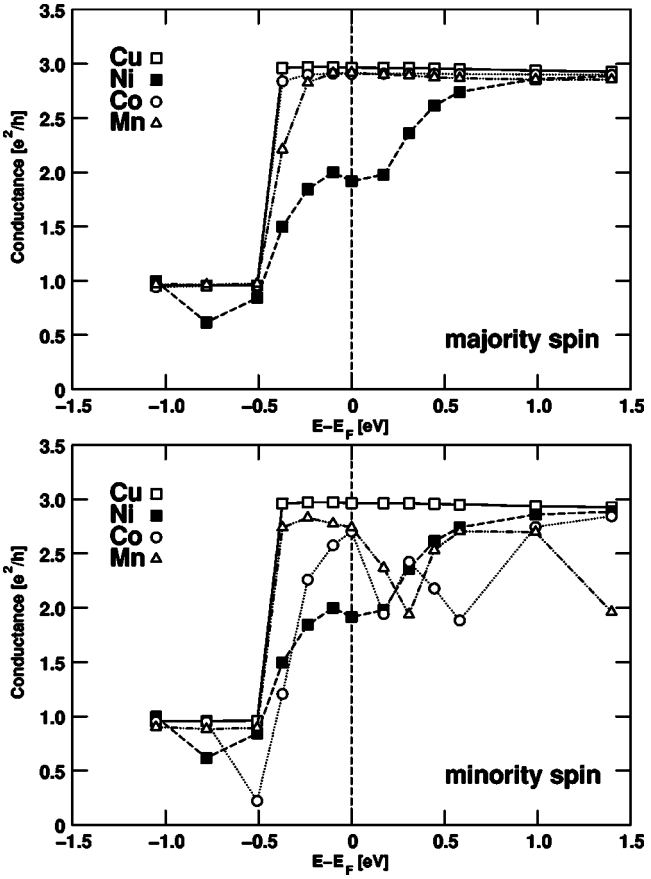

FIG. 9. Energy dependence of conductance for Ni, Co, Mn impurity pairs, together with the ideal wire conductance denoted by Cu.

by *d* states. The small drop in the Ni conductance at -0.7 eV is due to enhanced d_{xy} orbital character which was discussed also for the one impurity case. For the minority band we see large variations of the conductance with energy, on the other hand conductance is always above two channels for energies above E_F. Moreover, the rather small variation of the conductance at the E_F across the $3d$ series for the impurity pairs seen in Fig. 7 can be characterized as accidental.

The energy variation of g depends on the geometry of the defect and the wire atoms, since the orbital splitting depends strongly on the wire and the defect geometry. This strong energy and structure variation would cause a broadening in the peak structures seen for integer values of the conductance quantum in break junction experiments.

Eventually comparing the single defects with the defect pairs, we could conclude that a single defect might block the conducting channels more effectively than the defect pair. This is very pronounced in the case of Co where the drop in the conductance is larger for a single Co impurity compared to the Co pair, and it is also true for the other defects. The scattering is stronger if the *d*-impurity state is more localized. The localization is decreased by interference in the case of a defect pair.

IV. CONCLUSIONS

We have studied the scattering of ballistic electrons of thin Cu wires at transition-metal defects. Conductance is reduced for energies at the *d*-resonance state for a single impurity in the wire, and for spin-polarized transition-metal impurities conductance is different for the two-spin channels which leads to a spin-filter effect. Interference effects in a defect pair result in the formation of bonding and antibonding orbital splitting which depends sensitively on the geometric arrangement of the defects and causes a complicated variation of the conductance with energy and structure. Overall for the Cu 2×2 wire a single defect is seen to cause a larger reduction in conductance compared to the defect pair.

ACKNOWLEDGMENTS

We would like to thank the DFG, FG404 for financial support and P.H. Dederichs for helpful discussions.

[1] G.Y. Tseng and J.C. Ellenbogen, Science **294**, 1293 (2001).
[2] R. Landauer, IBM J. Res. Dev. **1**, 223 (1957); M. Büttiker, Phys. Rev. Lett. **57**, 1761 (1986).
[3] G. Rubio, N. Agrait, and S. Vieira, Phys. Rev. Lett. **76**, 2302 (1996).
[4] H. Ohnishi, Y. Kondo, and K. Takayanagi, Nature (London) **395**, 780 (1998).
[5] J.M. Krans, J.M. van Ruitenbeek, V.V. Fisun, I.K. Janson, and L.J. de Jongh, Nature (London) **375**, 6534 (1995).
[6] E. Scheer, N. Agrait, J.C. Cuevas, A.L. Yeyati, B. Ludoph, A. Martin-Rodero, G.R. Bollinger, J.M. van Ruitenbeek, and C. Urbina, Nature (London) **394**, 154 (1998).
[7] V. Rodrigues, T. Fuhrer, and D. Ugarte, Phys. Rev. Lett. **85**, 4124 (2000).
[8] V. Rodrigues, J. Bettini, A.R. Rocha, L.G.C. Rego, and D. Ugarte, Phys. Rev. B **65**, 153402 (2002).
[9] M. Brandbyge, J. Schiotz, M.R. Sorensen, P. Stoltze, K.W. Jacobsen, J.K. Norskov, L. Olesen, E. Laegsgaard, I. Stensgaard, and F. Besenbacher, Phys. Rev. B **52**, 8499 (1995); J.L. Costa-Krämer, N. Garcia, N. Garcia-Mochales, P.A. Serena, M.I. Marques, and A. Correia, *ibid.* **55**, 5416 (1997); K. Hansen, E. Laegsgaard, I. Stensgaard, and F. Besenbacher, *ibid.* **56**, 2208 (1997).
[10] A. Enomoto, S. Kurokawa, and A. Sakai, Phys. Rev. B **65**, 125410 (2002).
[11] N. Demoncy, O. Stephan, B. Brun, C. Colliex, A. Loiseau, and H. Pascard, Eur. Phys. J. B **4**, 147 (1998).
[12] T. Thurn-Albrecht, J. Schotter, G.A. Kästle, N. Emley, T. Shibuachi, L. Krusin-Elbaum, K. Guarini, C.T. Black, M.T. Tuominen, and T.P. Russel, Science **290**, 2126 (2000).
[13] B.H. Hong, S.C. Bae, C.-W. Lee, S. Jeong, and K.S. Kim, Science **294**, 348 (2001).

[14] M.B. Nardelli, J.-L. Fattebert, and J. Bernholc, Phys. Rev. B **64**, 245423 (2001).
[15] N.D. Lang, Phys. Rev. B **52**, 5335 (1995).
[16] S.T. Pantelides, M. Di Ventra, and N.D. Lang, Physica B **296**, 72 (2001).
[17] M. Di Ventra and N.D. Lang, Phys. Rev. B **65**, 045402 (2001).
[18] N. Kobayashi, M. Aono, and M. Tsukada, Phys. Rev. B **64**, 121402(R) (2001).
[19] J.C. Cuevas, A.L. Yeyati, and A. Martín-Rodero, Phys. Rev. Lett. **80**, 1066 (1998).
[20] J.C. Cuevas, A.L. Yeyati, A. Martín-Rodero, G.R. Bollinger, C. Untiedt, and N. Agraït, Phys. Rev. Lett. **81**, 2990 (1998).
[21] M. Brandbyge, N. Kobayashi, and M. Tsukada, Phys. Rev. B **60**, 17064 (1999).
[22] M. Brandbyge, J.-L. Mozos, P. Ordejòn, J. Taylor, and K. Stokbro, Phys. Rev. B **65**, 165401 (2002).
[23] J. Taylor, H. Guo, and J. Wang, Phys. Rev. B **63**, 121104(R) (2001).
[24] D.J. Bakker, Y. Noat, A.I. Yanson, and J.M. van Ruitenbeek, Phys. Rev. B **65**, 235416 (2002).
[25] A. Rochefort and P. Avouris, L. Phys. Chem. A **104**, 9807 (2000).
[26] M. Brandbyge, K.W. Yacobsen, and J.K. Norskov, Phys. Rev. B **55**, 2637 (1997).
[27] I. Mertig, Rep. Prog. Phys. **62**, 237 (1999).
[28] N. Papanikolaou, R. Zeller, and P.H. Dederichs, J. Phys.: Condens. Matter **14**, 2799 (2002).
[29] P. Hohenberg and W. Kohn, Phys. Rev. **136**, B864 (1964); W. Kohn and L.J. Sham, *ibid.* **140**, A1133 (1965).
[30] S.H. Vosko, L. Wilk, and N. Nusair, Can. J. Phys. **58**, 1200 (1980).
[31] H.U. Baranger and A.D. Stone, Phys. Rev. B **40**, 8169 (1989).
[32] P. Mavropoulos, N. Papanikolaou, and P. H. Dederichs (unpublished).
[33] H. Mehrez, J. Taylor, H. Guo, J. Wang, and C. Roland, Phys. Rev. Lett. **84**, 2682 (2000).
[34] D. Orlikowski, H. Mehrez, J. Taylor, H. Guo, J. Wang, and C. Roland, Phys. Rev. B **63**, 155412 (2001).